Proceedings for the 13th International Winds Workshop
27 June - 1 July 2016, Monterey, California, USA

STATUS OF OPERATIONAL AMVS FROM FENGYUN-2 SATELLITES

Xiaohu Zhang, Jianmin Xu, Qisong Zhang

National Satellite Meteorological Center
China Meteorological Administration, Beijing 100081, CHINA

Abstract

This paper briefly introduces status of AMVs operations at NSMC. Since the 12th International Winds Workshop (IWW12) held in June 2014, CMA continues AMVs operations and services. At present, FY-2G (105°E) and FY-2E (86.5°E) are both in operation. AMVs derivations are performed for both FY-2G and FY-2E. For FY-2G, AMVs are provided at 00 06 12 18 UTC, while FY-2E at 03 09 15 21 UTC. The wind derivation scopes are in the regions of satellite zenith angle less than 60 degree. There are several changes at the Fengyun-2 operational AMVs derivation system in the last two years. The algorithms mentioned last workshop, such as "second tracking", had been operational in the past two years. The BUFR encoder had been updated from BUFR edition 3 to 4. The QI without NWP had been added to Fengyun-2 AMVs.

In addition, this paper introduces the progress of Fengyun-2 AMVs historical dataset reprocessing and Fengyun-4 AMVs.

1. INTRODUCTION

Since the 12th International Winds Workshop (IWW12), there are several changes at the Fengyun-2 operational AMVs derivation system. The algorithms mentioned in IWW12, such as "second tracking", had been operational in the past two years. The BUFR encoder had been updated from BUFR edition 3 to 4. The QI without NWP had been added to Fengyun-2 AMVs. Finally, this paper introduces the progress of Fengyun-2 AMVs historical dataset reprocessing and Fengyun-4 AMVs.

2. ATMOSPHERIC MOTION VECTOR PRODUCTS GENERATED AT NSMC/CMA

Since the previous International Winds Workshop, FY-2G (105°E) and FY-2E (86.5°E) are both in operation. Infrared and water vapour channel AMV derivations are performed. For FY-2G, AMVs are provided at 00 06 12 18 UTC, while for FY-2E at 03 09 15 21 UTC. AMVs passed quality control are transmitted through GTS in BURF code. FY-2F is a backup satellite to FY-2G at 112°E and makes regional rapid scan as required. Table 1 Shows the NSMC/CMA wind products from the Fengyun satellites.

Product	Satellite	Nadir longitude	Product times
Infrared and Water Vapour Winds	FY-2G	105˚E	At 00:00,06:00,12:00,18:00(UTC)
Infrared and Water Vapour Winds	FY-2E	86.5˚E	At 03:00,09:00,15:00,21:00(UTC)
Infrared and Water Vapour Winds	FY-2F	112˚E	At 03:00,09:00,15:00,21:00(UTC)

Table 1: **The CMA wind products from the Fengyun satellites**

FY-2G/FY-2E winds are compared with ECMWF global atmospheric reanalysis data. The comparisons are made for the years of 2013 and 2015. Table 2 and table 3 are respectively mean and standard deviation of departures from FY-2G/FY-2E wind speed and reanalysis winds for IR and WV channels. The comparison results are in unit m/s. The result shows that the mean and STD of IR and WV AMVs have a little improvement except the STD of WV AMVs.

	High level IR winds (Above 400hPa)		Middle level IR winds (between 400-700hPa)		Low level IR winds (below 700hPa)		Water Vapor Winds	
	2013	2015	2013	2015	2013	2015	2013	2015
Jan	-1.94	-1.37	-3.90	-2.54	-0.58	0.10	-0.38	-0.37

Feb	-1.94	-1.37	-3.06	-2.58	-0.31	-0.14	-0.41	-0.37
Mar	-2.21	-1.25	-2.69	-2.45	-0.36	0.07	-0.44	-0.25
Apr	-2.76	-1.04	-3.17	-2.16	-0.32	0.13	-0.66	-0.04
May	-2.61	-1.08	-2.63	-2.11	-0.08	-0.15	-0.68	-0.08
Jun	-2.70	-1.09	-2.50	-1.84	-0.17	0.22	-0.61	-0.09
Jul	-2.92	-1.15	-2.74	-2.24	-0.26	-0.21	-0.62	-0.15
Aug	-2.85	-1.12	-3.28	-1.99	-0.26	-0.25	-0.49	-0.12
Sep	-2.90	0.10	-3.10	-1.92	-0.19	-0.19	-0.54	0.10
Oct	-2.46	-1.01	-2.67	-2.11	-0.35	-0.24	-0.36	-0.01
Nov	-2.26	0.07	-3.54	-2.04	-0.22	0.03	-0.43	0.07
Dec	-2.08	0.11	-3.86	-2.28	-0.31	0.16	-0.42	0.11

Table 2: **Mean of departures between FY-2G/FY-2E and reanalysis wind speed (QI>0.8)**

	High level IR winds (Above 400hPa)		**Middle level IR winds (between 400-700hPa)**		**Low level IR winds (below 700hPa)**		**Water Vapor Winds**	
	2012	**2013**	**2012**	**2013**	**2012**	**2013**	**2012**	**2013**
Jan	4.64	4.61	6.04	5.14	3.02	2.64	4.26	4.61
Feb	4.72	4.36	6.01	5.06	3.12	2.76	4.28	4.36
Mar	4.81	4.61	5.81	4.65	2.74	2.45	3.90	4.61
Apr	4.91	4.39	5.79	4.43	2.70	2.35	3.95	4.39
May	4.88	4.51	5.65	4.50	2.66	2.50	3.95	4.51
Jun	4.94	4.57	5.40	4.62	2.53	2.56	4.25	4.57
Jul	5.06	4.76	5.50	4.54	2.80	2.55	4.62	4.76
Aug	5.03	4.67	5.52	4.20	2.79	2.49	4.17	4.67
Sep	4.96	4.51	5.62	4.36	2.88	2.55	4.05	4.51
Oct	4.85	4.28	5.71	4.38	2.83	2.63	3.90	4.28
Nov	4.50	4.16	5.61	4.44	2.75	2.49	3.71	4.16
Dec	4.50	4.34	5.96	4.47	3.11	3.62	4.17	4.34

Table 3: **STD of departures between FY-2G/FY-2E and reanalysis wind speed (QI>0.8)**

3. CHANGES IN OPERATIONAL SYSTEM

Several R&D algorithms mentioned in IWW12 were applied to AMVs operational system at CMA successively in the last two years. The quality of AMVs in 2015 had increased.

R&D algorithm (mentioned in IWW12)	**Time (in operation)**
A new calibration system	Mar.2013
Eliminate the influence of abnormal satellite image	Oct.2014
Remove noise in the satellite image	Oct.2014
Second tracking algorithm	Nov.2014
Height assignment in inversion layer	Dec.2014
Height assignment in target box full of cloud	Dec.2014

Table 4: **Algorithms applied to AMVs' operational system in last two years**

The BUFR encoder had been updated from BUFR edition 3 to 4. The QI without NWP had been added to Fengyun-2 AMVs.

3.1 Calibration Improvement

A new calibration system called CIBLE was updated to AMVs operational system in last two years. The CIBLE method has been independently developed by using both lunar calibration (LC) and inner-blackbody calibration (IBBC) for TEBs, which is widely considered to be a prominent progress in terms of operational calibration for FY-2 satellite. The CIBLE software has been operational working in ground segments of FY-2F, FY-2E and FY-2D satellites since July 21, 2012, March 27 and May 21, 2013 respectively.

By using the latest CIBLE outcomes, the performance of AMV has also been greatly improved. Particularly, it is validated by ECMWF that the RMSE of WV-AMV for FY-2E satellite remains 4-5 m/s and the bias of IR-AMV for FY-2D satellite has been decreased by about 1.5 m/s after using CIBLE approaches.

3.2 Image navigation improvements

In some special period, abnormal images were taken. The examples of abnormal images may due to direct sunshine, sun transit outage, and moon influence and so on. Some abnormal satellite image may affect the image navigation and then AMVs quality. Figure 1 shows examples of abnormal images.

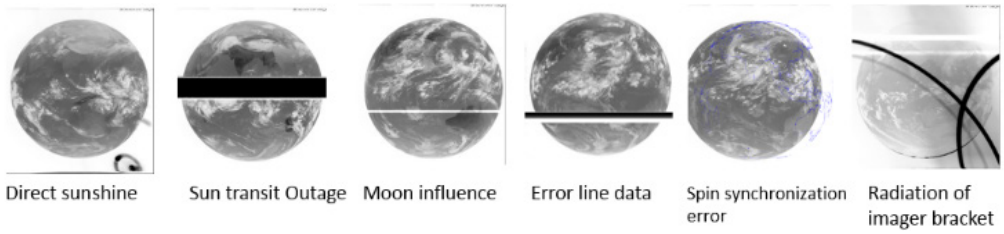

Figure 1: **Examples of abnormal images**

A quality control algorithm is performed to catch correct observation vectors toward earth centre and to eliminate the influence of abnormal satellite image. Figure 2 presents an example of an abnormal image and the result of the quality control algorithm. The figure in left is an abnormal image with direct sunshine. The figure in right is the time series of observation vectors toward earth centre (the upper part shows the line number of disc centre; the lower part shows the column number of disc centre). For the figures in right, red points are the time series of disc centre without using the quality control algorithm which is not continuous; blue points are after quality control which is smoother than the red. Using blue points, better image navigation is reached.

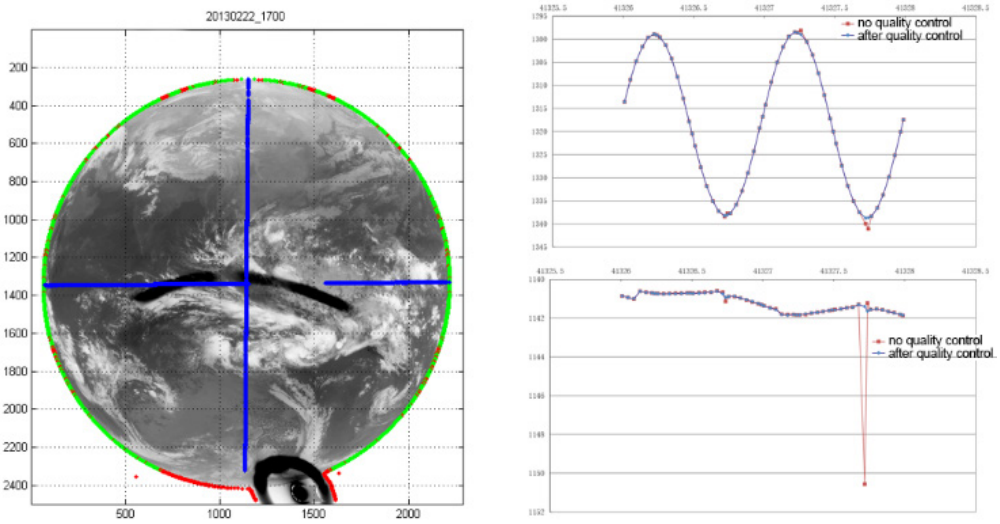

Figure 2: **Example of an abnormal image and the result of the quality control algorithm**

3.3 Remove noise points from satellite imagery

During the operation of AMVs, some noise data were found in the FY-2E image. The noise data are in both infrared and water vapour channel. The noise data may influence the quality of AMVs. An algorithm based on median filter is performed to identify and eliminate the noise. In figure 3 and 4, there are noise points in the left images, after filtering the noise points are removed in the right images. Figure 5 shows AMVs from Water vapor channel image with noise and image removed noise; in the left, due to the influence of noise, the wind field cannot be calculated around the noise, which leads to the discontinuity of the wind field; the corresponding position in the right, the wind field are continuous because the noise point is eliminated.

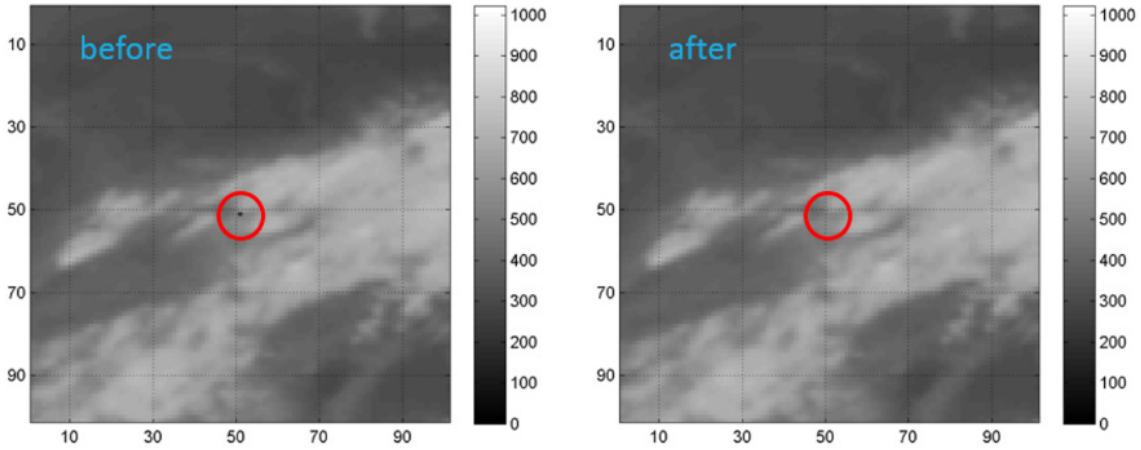

Figure 3: **Infrared channel image with noise and result image removed noise**

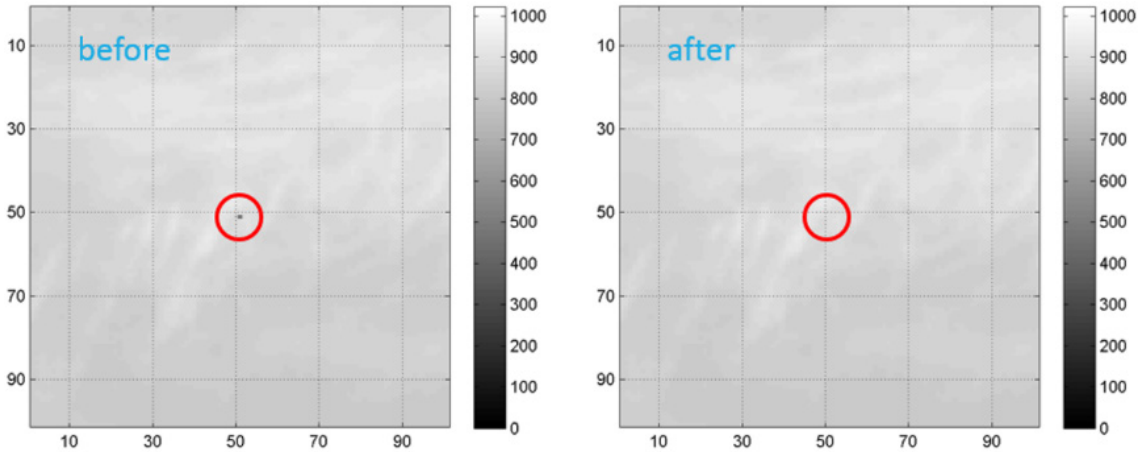

Figure 4: **Water vapour channel image with noise and result image removed noise**

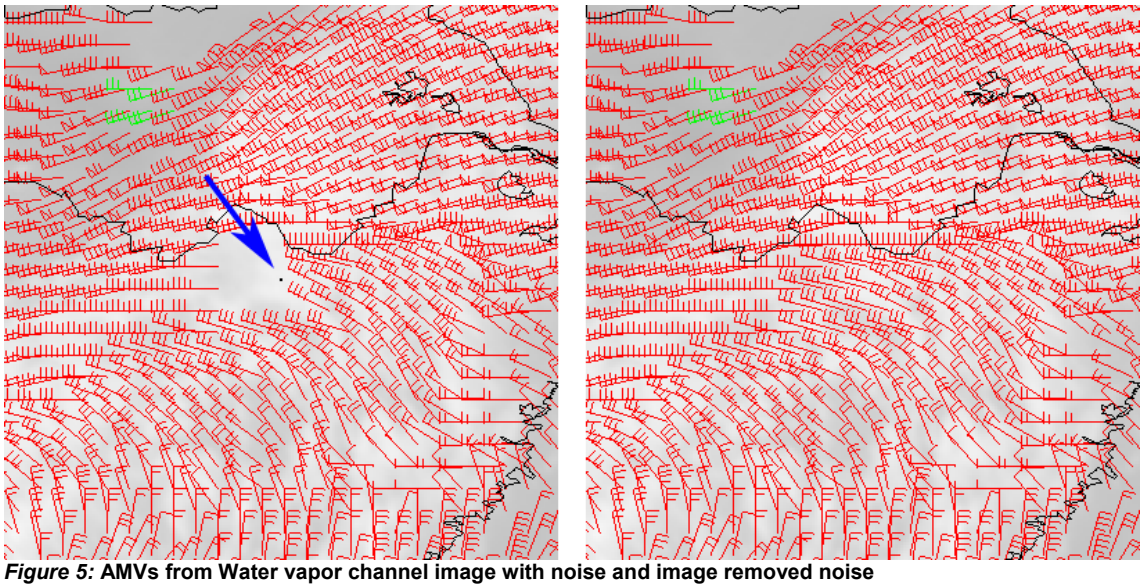

Figure 5: **AMVs from Water vapor channel image with noise and image removed noise**

3.4 Second tracking

In order to obtain more accurate wind speed, if the correlation coefficient of first tracking is larger than 0.8, second tracking will be performed. The first tracking box is 32 X 32, and the second tracking box is 16 X 16. Figure 6 shows an example of second tracking; the green points represent AMVs successfully performed in

the second tracking. For tracing targets performing second tracking, mean speed at first tracking is 11.01 m/s, while the second tracking 13.70 m/s.

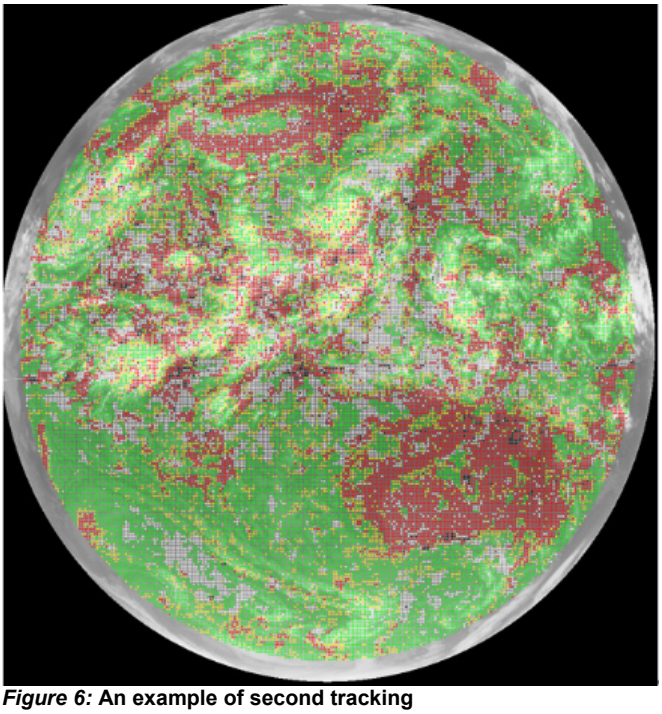

Figure 6: **An example of second tracking**

3.5 Height assignment in the region with low level inversion

In height assignment for semi-transparent clouds, it is important to define clear sky surface point in IR/WV scatter diagram. Normally surface points should have the highest WV temperature. But in the region with low level inversion, the highest WV temperature in the target box may represent top of the low-level inversion. This phenomenon was indicated by Takahito and Oyama (2008). For that region, it is tried to find clear sky WV temperature at surface. The surface point rather than top of the inversion is used to make semi-transparent cloud height assignment. Figure 7 shows a schematic diagram. The left figure shows low level inversion; the right figure is the IR/WV scatter diagram which is used to make semi-transparent cloud height assignment in the region with low level inversion. In the right figure, the surface point is defined at B rather than A. B represents surface, while A represents WV temperature at the top of the inversion.

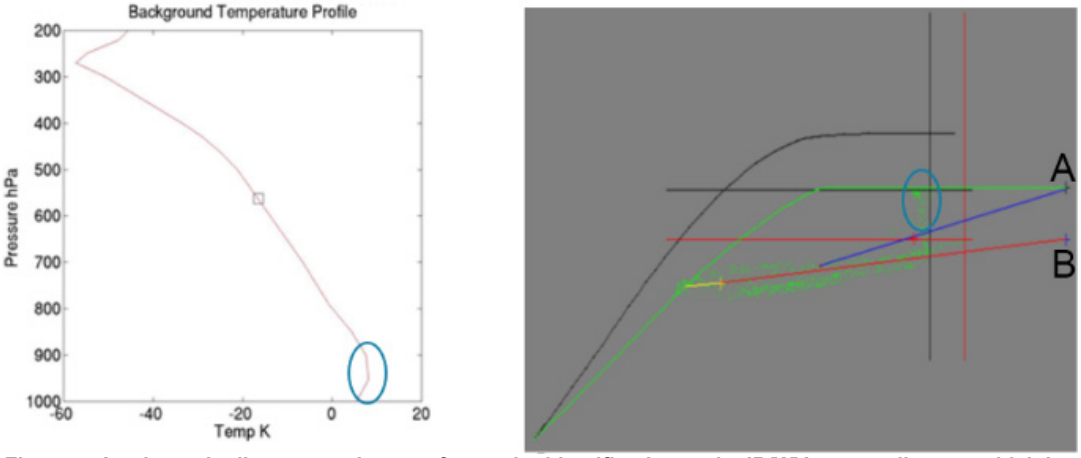

Figure 7: **A schematic diagram to show surface point identification at the IR/WV scatter diagram which is used to make semi-transparent cloud height assignment**

3.6 Height assignment for target box full of clouds

If the target box is full of cloud, a stepwise search procedure is performed to find clear sky surface point near the tracer. Figure 8 shows a schematic diagram. In the left figure, it is shown that the highest WV temperature in the search box does not represent surface. In the right figure, search box is expanded step by step to find the clear sky surface point. By expanding the area, the highest temperature may not just under the search area. But this is better than using highest WV temperature in cloud region to represent the one at surface.

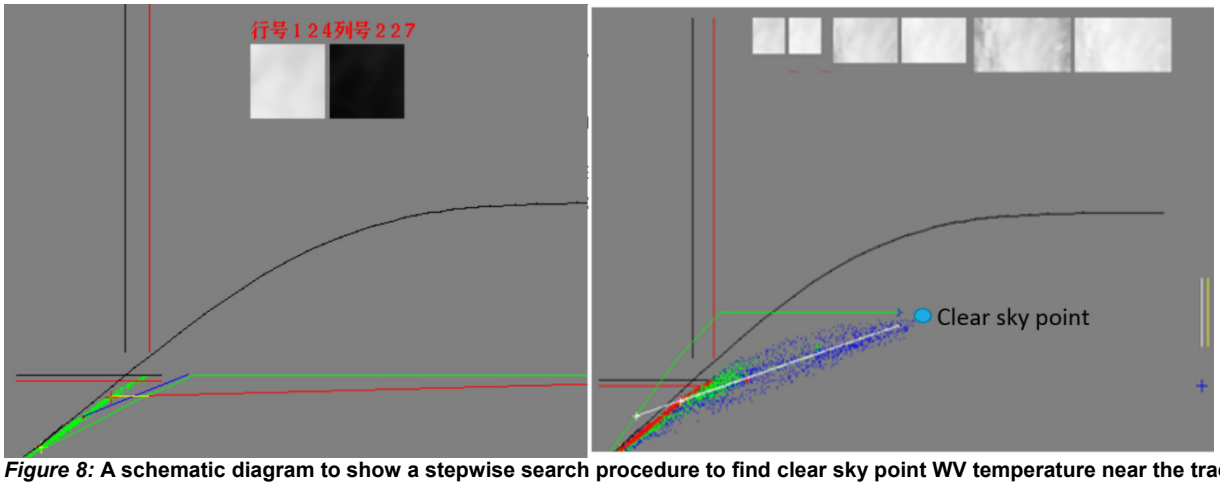

Figure 8: **A schematic diagram to show a stepwise search procedure to find clear sky point WV temperature near the tracer**

3.7 Changes in AMV BUFR data of CMA since last IWWG

The QI without NWP information was put in expanded data descriptor from 233 to 254 for both infrared and water vapor, and the satellite derived wind computation method (0 02 023) was put with 3 or 5 instead of 7 for water vapor wind.
Water vapour tracers with contribution to motion. Using clustering algorithm, if their WV BT are less than 235K and ΔIR-WV less than 15K, they are cloudy winds. Otherwise they are clear sky winds.

4. HISTORICAL DATASET REPROCESSING PROGRESS

CMA already started an project to reprocess the historical AMVs dataset in 2013. In this plan, all historical AMVs data will be reprocessed with the latest AMVs algorithm (CMA Version 2014). The project was undertaken and will be finished by the end of 2016.
Table 5 shows historical AMVs data in reprocess plan which include three Fengyun satellites from 2006 to 2013. The reprocessing job includes re-calibration, re-navigation, eliminate image noise and process AMVs with latest algorithm.

Satellites	Nadir Longitude	Date	AMVs Time (UTC)
FY-2C	105°E	Jan 1st, 2006 – Nov 24th, 2009	00/06/12/18
FY-2D	86.5°E	Feb 14th, 2007 – Dec 31st, 2013	03/09/15/21
FY-2E	105°E	Nov 23rd, 2009 – Dec 31st, 2013	00/06/12/18

Table 5: **The historical AMVs data in reprocessing plan**

5. FUTURE PLAN

5.1 CMA geostationary satellites status and plan

Figure 9 presents the CMA geostationary satellite configuration for 2015 – 2017.
FY-2G was launched in December 2014 and replaced FY-2E at 105°E in June 2015.
FY-2E drifted to 86.5°E and replace FY-2D in June 2015.

FY-2D drifted to 123.5°E and are no longer operational.
FY-2F will continue to be a hot standby satellite and provides regional rapid scan service.
FY-4A will be launched in Dec. 2016, located at 99.5˚E.

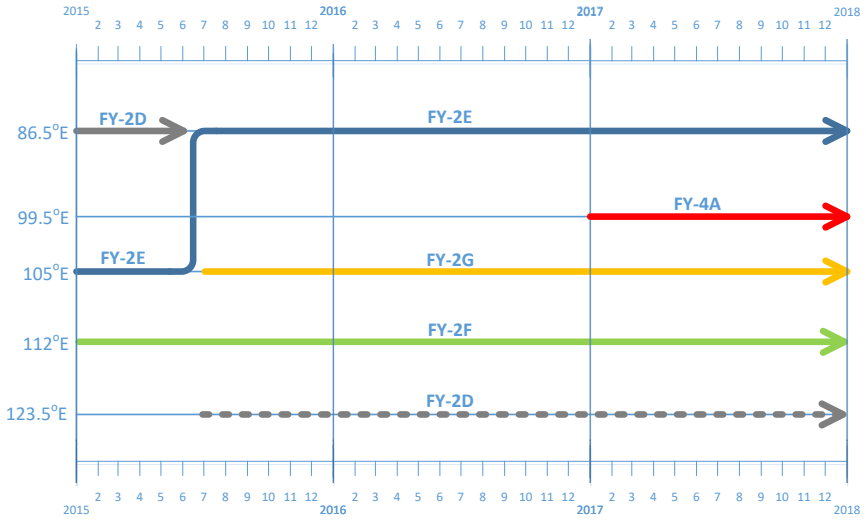

Figure 9: **The CMA geostationary satellite configuration for 2015 – 2017**

5.2 Introduction of FY-4A satellite

FY-4 is a new geostationary meteorological satellite series planned to cover the duration of 2016~2025. FY-4A is the first satellite of FY-4 series, is R&D satellite. Four new instruments are on board the FY-4A: Advanced Geosynchronous Radiation Imager (AGRI), Geosynchronous Interferometric Infrared Sounder (GIIRS), Lightning Mapping Imager (LMI) and Space Environment Package (SEP). FY-4A will be launched in Dec.2016.

5.3 FY-4A AGRI and AMVs

Table 6 shows channel feature of FY-4A AGRI and channels selected for derivation for AMVs.

Channel	Band(um)	Spatial Resolution	AMVs
Visible & Near-Infrared	0.45~0.49	1	
	0.55~0.75	0.5~1	
	0.75~0.90	1	VIS winds
Short-wave Infrared	1.36~1.39	2	
	1.58~1.64	2	
	2.10~2.35	2~4	
Mid-wave Infrared	3.5~4.0	2	
	3.5~4.0	4	
Water Vapor	5.8~6.7	4	clear sky and cloudy winds
	6.9~7.3	4	clear sky and cloudy winds
Long-wave Infrared	8.0~9.0	4	
	10.3~11.3	4	IR winds
	11.5~12.5	4	
	13.2~13.8	4	

Table 6: **channel feature of FY-4A AGRI and channels selected for derivation for AMVs.**

REFERENCES

Borde R.， Oyamma R., 2008, A Direct Link between Feature Tracking and Height Assignment of Operational Atmospheric Motion Vectors, 9th International Winds Workshop, Annapolis, Maryland, USA, 14-18

Feng Lu, Xiaohu Zhang, and Jianmin Xu, 2008, Image Navigation for the FY2 Geosynchronous Meteorological Satellite, Journal of Atmospheric and Oceanic Technology, 25, No. 7, 1149—1165
Schmetz J，Arriaga A，Holmlund K，1998，Sensitivity of the height allocation of thin cloud tracers in satellite calibration，Proceedings of the 4th International Winds Workshop，Saanenmöser，Switzerland，20 – 23 October 1998，EUMETSAT Publication，EUM P24：225-231
Szejwach G，1982，Determination of semitransparent cirrus cloud temperature from infrared radiances：application to meteosat，Journal of Applied Meteorology，21(3)：384-393
Takahito I. and Oyama R., 2008, Developments for Quality Improvement of Atmospheric Motion Vectors Product, Meteorological Satellite Center Technical Note, No.51, pp55
Xu Jianmin， Zhang Qisong，1996，Calculation of cloud motion wind with GMS-5 images in China，Proceedings of the Third International Winds Workshop，Ascona，10-12 June 1996，EUMETSAT Publication，EUM P18： 45-52
Xu J，Holmlund K，Zhang Q，Schmetz J，2002，Comparison of two schemes for derivation of atmospheric motion vectors，Journal of Geophysical Research，107(D14)
Xu Jianmin，Zhang Qisong，etc. ，2004, Recent works aimed at operational FY2C AMVS，Proceedings of the 7th International Winds，Helsinki，Finland，14-17 June，2004
Xu Jianmin，Zhang Qisong，Zhang Xiaohu，Wang Sujuan，Lu Feng，Status of operational AMVs from FY-2C，Proceedings of the 8th International Winds Workshop，Beijing，China，24-28 April，2006
Zhang Xiaohu，Xu Jianmin，Two applications of improvements for AMVs of NSMC/CMA-- re-navigation based on full earth disk image & calibration of radiation transfer using NWP data，Proceedings of the 10th International Winds Workshop，Tokyo，Japan，22-2